fractal and fractional

MDPI

Article

Global Mittag-Leffler Attractive Sets, Boundedness, and Finite-Time Stabilization in Novel Chaotic 4D Supply Chain Models with Fractional Order Form

Muhamad Deni Johansyah [1,*], Aceng Sambas [2,3], Muhammad Farman [4,5], Sundarapandian Vaidyanathan [6], Song Zheng [7,8], Bob Foster [9] and Monika Hidayanti [1]

[1] Department of Mathematic, Universitas Padjadjaran, Jatinangor, Sumedang 45363, Indonesia; monika.hidayanti@unpad.ac.id
[2] Faculty of Informatics and Computing, Universiti Sultan Zainal Abidin, Besut Campus, Besut 22200, Malaysia; acengsambas@unisza.edu.my or acengs@umtas.ac.id
[3] Department of Mechanical Engineering, Universitas Muhammadiyah Tasikmalaya, Tasikmalaya 46196, Indonesia
[4] Department of Mathematics, Faculty of Arts and Sciences, Near East University, Nicosia 99138, Cyprus; farmanlink@gmail.com
[5] Department of Computer Science and Mathematics, Labanese American University, Beirut 1107-2020, Lebanon
[6] Centre for Control Systems, Vel Tech University, Avadi Chennai 600062, Tamil Nadu, India; sundar@veltech.edu.in
[7] School of Data Science, Zhejiang University of Finance and Economics, Hangzhou 310018, China; szh070318@zufe.edu.cn
[8] Institute of Mathematics and Interdisciplinary Sciences, Zhejiang University of Finance and Economics, Hangzhou 310018, China
[9] Faculty of Business and Economics, Universitas Informatika dan Bisnis Indonesia, Bandung 40285, Indonesia; bobriset@unibi.ac.id
* Correspondence: muhamad.deni@unpad.ac.id

Citation: Johansyah, M.D.; Sambas, A.; Farman, M.; Vaidyanathan, S.; Zheng, S.; Foster, B.; Hidayanti, M. Global Mittag-Leffler Attractive Sets, Boundedness, and Finite-Time Stabilization in Novel Chaotic 4D Supply Chain Models with Fractional Order Form. *Fractal Fract.* **2024**, *8*, 462. https://doi.org/10.3390/fractalfract8080462

Academic Editor: António Lopes

Received: 26 June 2024
Revised: 31 July 2024
Accepted: 3 August 2024
Published: 6 August 2024

Abstract: This research explores the complex dynamics of a Novel Four-Dimensional Fractional Supply Chain System (NFDFSCS) that integrates a quadratic interaction term involving the actual demand of customers and the inventory level of distributors. The introduction of the quadratic term results in significantly larger maximal Lyapunov exponents (MLE) compared to the original model, indicating increased system complexity. The existence, uniqueness, and Ulam–Hyers stability of the proposed system are verified. Additionally, we establish the global Mittag-Leffler attractive set (MLAS) and Mittag-Leffler positive invariant set (MLPIS) for the system. Numerical simulations and MATLAB phase portraits demonstrate the chaotic nature of the proposed system. Furthermore, a dynamical analysis achieves verification via the Lyapunov exponents, a bifurcation diagram, a 0–1 test, and a complexity analysis. A new numerical approximation method is proposed to solve non-linear fractional differential equations, utilizing fractional differentiation with a non-singular and non-local kernel. These numerical simulations illustrate the primary findings, showing that both external and internal factors can accelerate the process. Furthermore, a robust control scheme is designed to stabilize the system in finite time, effectively suppressing chaotic behaviors. The theoretical findings are supported by the numerical results, highlighting the effectiveness of the control strategy and its potential application in real-world supply chain management (SCM).

Keywords: chaos theory; supply chain dynamics; control strategies; finite-time control; fractional order; Lyapunov exponents; Mittag-Leffler stability

1. Introduction

Fractional calculus, the extension of traditional calculus to non-integer orders, has found application across various fields due to its ability to model systems with memory and hereditary properties [1–3]. In control systems, fractional-order controllers like

the fractional PID provide enhanced performance and robustness, especially in complex dynamic systems [4]. Signal processing benefits from fractional Fourier transforms for time-frequency analysis, while biomedical engineering utilizes fractional calculus to model blood flow dynamics, tissue viscoelasticity, and drug delivery systems [5–7]. Material science and physics leverage fractional calculus to study viscoelastic materials, anomalous diffusion, and wave propagation in complex media, offering more accurate representations of these phenomena [8–10].

In economics, fractional calculus plays a crucial role in modeling and analyzing financial systems that exhibit memory and long-term dependencies [10,11]. It is used to model stock market dynamics and option pricing, accounting for the persistent and irregular behavior observed in financial time series [12–14]. Fractional Brownian motion provides a more accurate description of asset price movements, enhancing risk assessment and derivative pricing models [15,16]. Additionally, fractional calculus helps in understanding economic cycles, consumer behavior, and the diffusion of innovation over time, offering a comprehensive framework for the analysis of complex economic phenomena [17,18]. Its application extends to the modeling of interest rates, market volatility, and portfolio optimization, providing valuable insights for economists and financial analysts [19,20].

In recent years, the field of fractional calculus has seen significant development, particularly in its application to complex systems with memory effects and non-local boundaries. Notable studies include Al Fahel et al.'s [21] exploration of quadratic and cubic logistic models involving the Caputo–Fabrizio operator and Hegade and Bhalekar's stability analysis of Hilfer fractional-order differential equations [22], both of which underscore the relevance of fractional calculus in dynamic systems modeling. Additionally, Rahman et al. provided valuable insights into the modeling and analysis of implicit fractional-order differential equations with multiple first-order fractional derivatives [23]. Fractal theory further facilitates contemporary research, illustrating both theoretical advancements and practical applications across various scientific and engineering disciplines [24–26]. These recent contributions highlight the transformative potential of fractional calculus in providing sophisticated mathematical tools for the accurate description of complex phenomena.

In recent years, the study of supply chain dynamics has increasingly recognized the importance of incorporating chaos theory to understand and manage the inherent complexities and unpredictability within supply chain systems [27–29]. Traditional models often fall short in capturing the non-linear and dynamic nature of real-world supply chains, leading to inefficiencies and vulnerabilities [30]. In the context of supply chains, fractional calculus can capture the long-term dependencies and interactions between different components of the supply chain, which are often overlooked by integer-order models [31,32]. He et al. [33] developed a fractional-order digital manufacturing supply chain system using the Adomian decomposition method and explored its chaotic behavior through dynamical and complexity analyses. Yan et al. [34] created a mathematical model for a 4D supply chain incorporating a computer-aided digital manufacturing process and designed a stabilizing linear feedback controller for two dynamic scenarios within the supply chain. Xu et al. [35] introduced an adaptive fractional-order sliding mode controller to achieve chaos synchronization in supply chain systems facing market disruptions, significantly enhancing the understanding of chaotic supply chain networks and optimizing the management strategies. Cuong et al. [36] investigated the dynamical analysis and efficient management strategies of supply chain systems using a four-stage hyperchaotic Lorenz–Stenflo equation under disruptive conditions, demonstrating that their novel decision-making strategy provides valuable insights for the effective management of digital supply chain networks amid market volatility. However, four-dimensional supply chain models introduce another layer of complexity as they must account for the dynamic interactions between various interconnected elements within the system. This often demands more intensive computation and detailed data for model validation, posing significant challenges in both research and practical implementation. Therefore, despite its substantial potential for better understanding and management, these challenges have made research in this area relatively scarce.

Based on this issue above, this paper builds on the foundation laid by Xu et al. [35], who introduced a four-dimensional (4D) integrated chaotic supply chain model. The Xu model provided significant insights into the chaotic behavior of supply chains, demonstrating the potential for improved management strategies through chaos theory. However, there remains a need to further enhance the model to better reflect the complexities of supply chain interactions and to develop robust control mechanisms.

The main contributions and novelties of this paper are as follows.

- This work integrates a novel quadratic interaction term involving the actual customer demand and distributor inventory levels into the NFDFSCS. This addition significantly enhances the chaotic behavior and complexity of the SCM, as evidenced by the increased MLE compared to existing models.
- This study rigorously verifies the existence, uniqueness, and Ulam–Hyers stability of the proposed NFDFSCS. This theoretical validation ensures that the model is robust and reliable in capturing the complex dynamics of the NFDFSCS.
- This work establishes the MLAS and MLPIS for the NFDFSCS. These sets provide a comprehensive framework for understanding the long-term behavior and stability of the system.
- This work employs sophisticated dynamical analysis tools such as Lyapunov exponents, bifurcation diagrams, 0–1 tests, and complexity analysis. These methods demonstrate the chaotic nature of the system and provide deeper insights into the dynamic interactions within the supply chain model.
- A new numerical approximation method is proposed to solve non-linear fractional differential equations using fractional differentiation with a non-singular and non-local kernel. Additionally, a robust control scheme is designed to stabilize the NFDFSCS in finite time, effectively suppressing chaotic behaviors. The theoretical findings, supported by the numerical results, highlight the practical applicability of this control strategy in the NFDFSCS.

2. Basic Definition

Several important and useful discoveries regarding non-linear dynamics and contemporary calculus were described in [37].

Definition 1. *Given that $\gamma(t)$ is continuous and differentiable on the function $L^1([0,T],R)$, the Riemann–Liouville integral of fractional order $q \in (0,1)$ is defined as*

$$ {}_0^{RL}I_t^q(t) = \frac{1}{\Gamma(q)}\int_0^t (t-\xi)^{q-1}\gamma(\xi)d\xi, $$

where the integral on the right-hand side is pointwise defined on $(0,\infty)$.

Definition 2. *Given that $\gamma(t)$ is continuous on the function $[0,T]$, the Caputo derivative of $\gamma(t)$ is defined as*

$$ {}_0^{C}D_t^q\gamma(t) = \frac{1}{\Gamma(\theta-q)}\left[\int_0^t (t-\xi)^{\theta-q-1}\frac{d^\theta}{d\xi^\theta}\gamma(t)(\xi)d\xi,\right] $$

where $\Gamma(.)$ represents a Gamma function. When $\theta = 1$, the above equation reduces to

$$ {}_0^{C}D_t^q\gamma(t) = \frac{1}{\Gamma(\theta-q)}\left[\int_0^t (t-\xi)^{-q}\gamma'(t)(\xi)d\xi,\right] $$

The integral of the $\gamma(t)$ Caputo operator of fractional order $q \in (0,1)$ can be defined as

$$ {}^{C}I_t^q\gamma(t) = \frac{1}{\Gamma(q)}\int_0^t (t-q)^{q-1}d\xi. $$

Definition 3 ([38]). *Consider the Lyapunov function $V_\varpi(t) = V_\varpi(x(t))$ with $\varpi > 0$, and if there exist constants $L_\varpi > 0$, $r_\varpi > 0$ and $x_0 \in R^m$ such that*

$$V_\varpi(t) - L_\varpi \leq (V_\varpi(t_0) - L_\varpi)E_q(-r_\varpi(t - t_0)^q),$$

for $t \geq t_0$, $V_\varpi(t_0) > L_\varpi$, $V_\varpi(t) > L_\varpi$, then the set $\Psi_\varpi = \{x(t) \in R^m \ | V_\varpi(x(t)) \ \leq L_\varpi\}$ is said to be a global MLAS of the system. If, for any $t > t_0$, $x(t, t_0, x_0) \in \Psi_\varpi$, $t > t_0$, or $x_0 \in \Psi_\varpi$, then Ψ_ϖ is said to be an MLPIS, where $x(t) = (x_1, x_2, \cdots, x_m)^T$, $x_0 = x(t_0)$.

3. Modeling and Dynamics of the NFDFSCS

Xu et al. [35] described a 4D Chaotic Supply Chain Model (4DCSCM) via the following differential equations:

$$\begin{cases} \dot{y}_1 = -(y_2 + ny_1) \\ \dot{y}_2 = my_3 - (n+1)y_2 + cy_1 \\ \dot{y}_3 = ry_2 - y_3 - y_2y_4 \\ \dot{y}_4 = y_2y_3 - (1-k)y_4 \end{cases} \tag{1}$$

where the state variables y_1, y_2, y_3, y_4 are the actual demand of the customers, the retailer's demand order, the inventory level of the distributor, and the quantity produced by the manufacturer, respectively. With $c = 1.5$, $m = 3.5$, $n = 0.2$, $r = 26$, and $k = 0.3$, Xu et al. [35] observed a chaotic attractor for the 4DCSCM (1) for the initial state $Y_0 = (0.02, 0.02, 0.02, 0.02)$. For this case, the Lyapunov exponents of the Xu 4DCSCM (1) are obtained as

$$L_1 = 0.1730, L_2 = 0, L_3 = -0.5006, L_4 = -2.7728 \tag{2}$$

In this research work, we propose a new 4DCSCM by introducing a quadratic interaction term involving the actual demand of the customers (y_1) and the inventory level of the distributor (y_3) in the second differential equation describing the rate of change in the retailer's demand order. Thus, we propose the new 4DCSCM given by

$$\begin{cases} \dot{y}_1 = -(y_2 + ny_1) \\ \dot{y}_2 = my_3 - (n+1)y_2 - py_1y_3 + cy_1 \\ \dot{y}_3 = ry_2 - y_3 - y_2y_4 \\ \dot{y}_4 = y_2y_3 - (1-k)y_4 \end{cases} \tag{3}$$

We consider the values of the new 4DCSCM parameters as $c = 1.6$, $m = 3.6$, $n = 2$, $r = 27$, $k = 0.3$, and $p = 0.2$. We take the initial state as $Y_0 = (0.02, 0.02, 0.02, 0.02)$. For this case, the Lyapunov exponents of the new 4DCSCM (3) are obtained as

$$L_1 = 0.4920, L_2 = 0, L_3 = -2.5271, L_4 = -4.6654 \tag{4}$$

These results show that the new 4DCSCM (3) is chaotic and dissipative.

It is easy to see that the maximal Lyapunov exponent (MLE) of the new 4DCSCM (3) is significantly larger than the MLE of the Xu chaotic supply chain model (1). Hence, the proposed 4DCSCM (3) has greater complexity than the Xu 4DCSCM (1).

In Figure 1, the phase portraits of the proposed new 4DCSCM are shown. The inclusion of the novel quadratic interaction term involving the actual customer demand (y_1) and the inventory level of the distributor (y_3) significantly enhances the chaotic behavior of the system. This is evident from the phase portraits, where the complex dynamic interactions are vividly illustrated. Comparing these results to the model proposed by Xu et al. [35], there are notable differences in the complexity and chaotic nature of the systems. Xu et al. [35] introduced a 4D integrated chaotic supply chain model and observed chaotic attractors, which were used to improve the management strategies through chaos theory. However, the maximal Lyapunov exponents (MLE) of the new 4DCSCM (3) in our study

are significantly larger than those of the Xu model. This indicates the higher degree of complexity and chaos in our system.

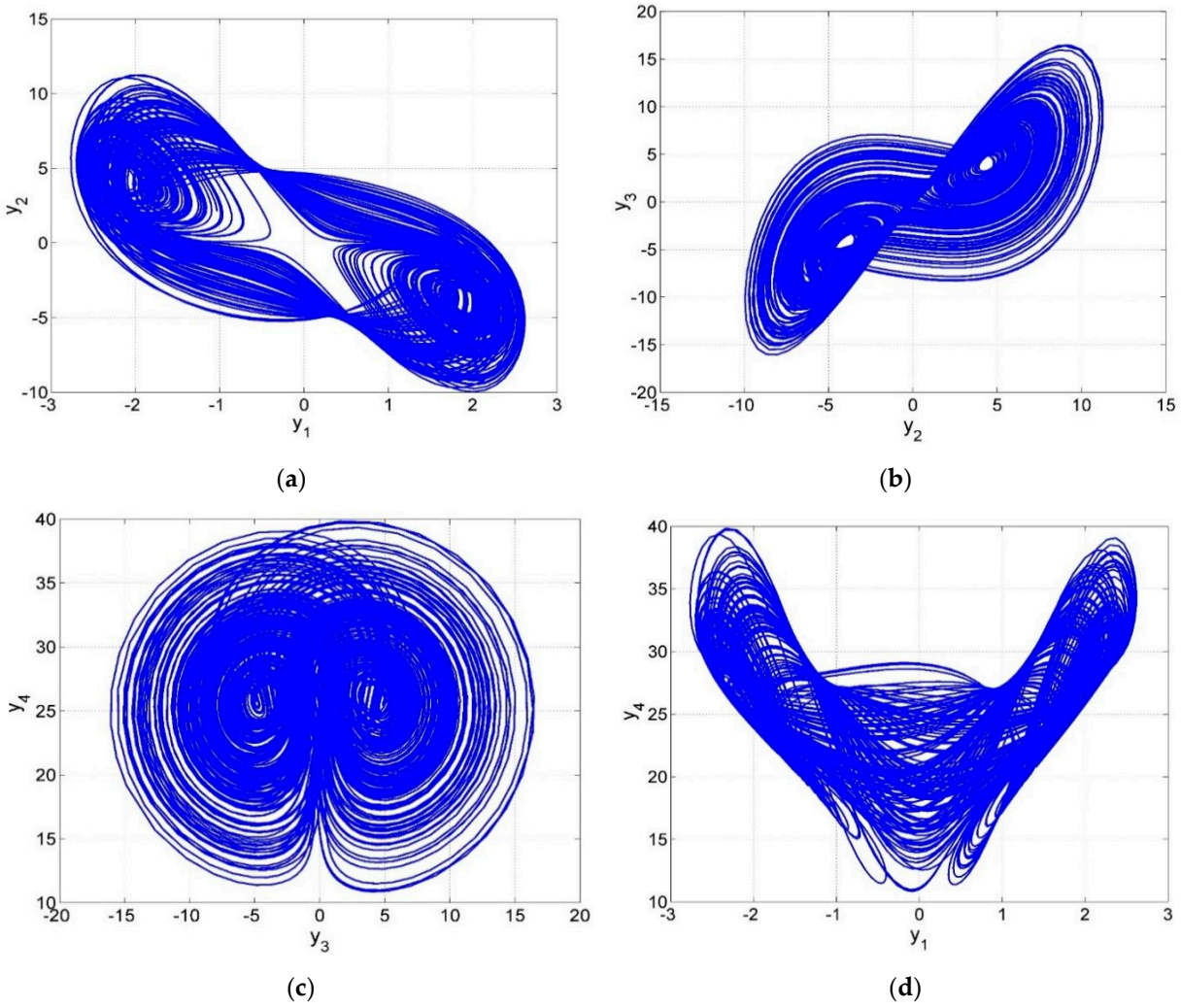

Figure 1. Phase portrait of the new 4DCSC system (3) using MATLAB: (**a**) $y_1 - y_2$ plane, (**b**) $y_2 - y_3$ plane, (**c**) $y_3 - y_4$ plane, and (**d**) $y_1 - y_4$ plane.

The enhanced chaotic behavior in our model can be attributed to the introduction of the quadratic interaction term, which was not present in the Xu et al. [35] model. This term intensifies the non-linear interactions between the state variables, leading to more complex dynamical behavior. The phase portraits in Figure 1 demonstrate this increased complexity, showing more intricate and dense trajectories compared to the simpler chaotic attractors observed by Xu et al. [35]. In summary, while both models exhibit chaotic behavior, the proposed 4DCSCM with the quadratic interaction term presents a higher degree of complexity and more pronounced chaotic dynamics than the model of Xu et al. [35]. This enhancement can potentially lead to better insights and more effective strategies for the management and optimization of supply chain systems.

This complexity serves to enhance our understanding of the chaotic dynamics within the supply chain rather than directly improving the predictive accuracy. The increased complexity highlights the need for robust and adaptive management strategies to effectively navigate the inherent unpredictability of the supply chain system.

By introducing the Caputo differential definition, the fractional order form of the dimensionless equation for the above circuit can be written as

$$\begin{cases} {}^{C}D_t^q y_1 = -(y_2 + ny_1), \\ {}^{C}D_t^q y_2 = my_3 - (n+1)y_2 - py_1y_3 + cy_1, \\ {}^{C}D_t^q y_3 = ry_2 - y_3 - y_2y_4, \\ {}^{C}D_t^q y_4 = y_2y_3 - (1-k)y_4. \end{cases} \tag{5}$$

This study rigorously verifies the existence, uniqueness, and Ulam–Hyers stability of the proposed system. These theoretical validations ensure that the model is robust and reliable in capturing the complex dynamics of supply chains. The global MLAS and MLPIS established for the system provide a comprehensive framework for understanding the long-term behavior and stability of the model.

3.1. Existence of the NFDFSCS (5)

We start by demonstrating that our problem has a solution. We apply fixed point theory for this. Let us define the Banach space $Y = A^4$ for our qualitative analysis, where $A = A(U, R)$ with

$$||N||_Y = \{y_1, y_2, y_3, y_4\}, \tag{6}$$

$$||N||_Y = max\{|\,T(t)\,| : t \in U\,\}, \tag{7}$$

given that $|\,N| = |y_1\,| + |y_2\,| + |y_3\,| + |y_4\,|$. The right side of the fractal fractional new 4DCSCM system is rewritten as

$$\begin{cases} W_1(t, N) = -(y_2 + ny_1), \\ W_2(t, N) = my_3 - (n+1)y_2 - py_1y_3 + cy_1, \\ W_3(t, N) = ry_2 - y_3 - y_2y_4, \\ W_4(t, N) = y_2y_3 - (1-k)y_4. \end{cases} \tag{8}$$

In this instance, the following system replaces the fractal fractional new 4DCSCM system

$${}^{C}D_t^q y_i = \gamma t^{\gamma-1} W_i(t, N), \tag{9}$$

and $i = 1, 2, 3, 4$ for all compartments. We rebuild our tree state system as the compact IVP in light of system

$$\begin{cases} {}^{C}D_t^q N(t) = \gamma t^{\gamma-1} W_i(t, N), \\ N(0) = N_0. \end{cases} \tag{10}$$

where $N(t) = (y_1, y_2, y_3, y_4)$, $N_0(t) = (y_{1,0}, y_{2,0}, y_{3,0}, y_{4,0})$, and $W(t, N) = W_1(t, N) + W_2(t, N) + W_3(t, N) + W_4(t, N)$.

Based on Equation (10), and by definition, we have

$$\frac{1}{\Gamma(\alpha - q)} \int_0^t \frac{\varphi^{\alpha}(\xi)}{(t-\xi)^{q-\alpha+1}} d\xi = W(t, N(t)) \tag{11}$$

The fractal fractional Caputo integral is applied to Equation (11), yielding

$$N(t) = N_0 + \frac{1}{\Gamma(q)} \int_0^t (t-\xi)^{q-1} W(\xi, N(\xi)) d\xi + \frac{(1-q)\gamma t^{\gamma-1} W(t, N(t))}{C(q)} \tag{12}$$

The expanded form of Equation (12) is Equation (5) provided by

$$\begin{cases} y_1 = y_1 + \frac{1}{\Gamma(q)} \int_0^t (t-\xi)^{q-1} W_1(\xi, N(\xi)) d\xi + \frac{(1-q)\gamma t^{\gamma-1} W_1(t, N(t))}{C(q)} \\ y_2 = y_2 + \frac{1}{\Gamma(q)} \int_0^t (t-\xi)^{q-1} W_2(\xi, N(\xi)) d\xi + \frac{(1-q)\gamma t^{\gamma-1} W_2(t, N(t))}{C(q)} \\ y_3 = y_3 + \frac{1}{\Gamma(q)} \int_0^t (t-\xi)^{q-1} W_3(\xi, N(\xi)) d\xi + \frac{(1-q)\gamma t^{\gamma-1} W_3(t, N(t))}{C(q)} \\ y_4 = y_4 + \frac{1}{\Gamma(q)} \int_0^t (t-\xi)^{q-1} W_4(\xi, N(\xi)) d\xi + \frac{(1-q)\gamma t^{\gamma-1} W_4(t, N(t))}{C(q)} \end{cases} \tag{13}$$

We now define the self-map $M : Y \to Y$ as follows to deduce a fixed-point problem

$$M(N(t)) = N_0 + \frac{1}{\Gamma(q)} \int_0^t (t-\xi)^{q-1} W(\xi, N(\xi)) d\xi + \frac{(1-q)\gamma t^{\gamma-1} W(t, N(t))}{C(q)}. \tag{14}$$

We apply the following Leray–Schauder theorem to demonstrate the existence of a solution to our fractal fractional new 4DCSCM (4).

Theorem 1 (Finite point theorem of Leray–Schauder [39]). *Let $H \subseteq Y$ be an open set with $0 \in P, P \subseteq H$ a closed convex and bounded set, and Υ a Banach space. Next, with respect to the continuous and compact mapping $M : \hat{P} \to H$, either*

A. $y \in \hat{P}$ exists such that $y = M(y)$; otherwise,
B. $y = \mu M(y)$ exists for any $y \in \partial P$ and $\mu \in (0,1)$.

The NFDFSCS (5) is limited in its existence since it simulates a real-world issue. These limitations, which are represented as (*C*) and (*D*) in Theorem 2, are essential in determining the dynamics and properties of the system. To define and control the behavior of the NFDFSCS (5) within the bounds of pragmatism and realism, (*C*) and (*D*) are in fact essential. Acknowledging these limitations is crucial to ensuring the thorough comprehension of the system and creating successful tactics.

Theorem 2. *Suppose that $W \in A(U \times Y, Y)$. If so,*

A. There exists $\lambda \in L^1(U; R^+)$ and then there exists $\xi \in A([0;\infty);(0;\infty))$, where it is non-decreasing such that, for all $t \in U$ and $N \in Y$,

$$|(t, N(t)| \leq \alpha(|N(t)|)\lambda(t). \tag{15}$$

B. Then, there exists $\vartheta > 0$, $\mu \in (0,1)$, such that

$$\frac{\vartheta}{N_0 + \left[\frac{(1-q)\gamma t^{\gamma-1}}{C(q)} + \frac{q\gamma t^{\gamma-1+q}\Gamma(\gamma)}{C(q)\Gamma(q+\gamma)}\right]\lambda_0^* \alpha(\vartheta)} > 1. \tag{16}$$

Given $\lambda_0^* = sup_{t\in U} |\lambda(t)|$, the NFDFSCS (5) may be solved.

Proof. Let us first take $M : Y \to Y$, as defined by Equation (14), and make the following assumptions,

$$Q_r = \{N \in Y : ||N||_Y \leq r\},$$

for a certain $r > 0$. It is obvious that, since Q is continuous, so is M. Given (A), we obtain

$$\begin{aligned}|M(N(t))| &\leq |N_0| + \frac{1}{\Gamma(q)}\int_0^t (t-\xi)^{q-1}|W(\xi, N(\xi))|d\xi + \frac{q\gamma t^{\gamma-1}|W(t, N(t))|}{C(q)} \\ &\leq |N_0| + \frac{1}{\Gamma(q)}\int_0^t (t-\xi)^{q-1}\lambda(\xi)\alpha(|N(\xi)|)d\xi + \frac{q\gamma t^{\gamma-1}\lambda(t)\alpha(|N(t)|)}{C(q)} \\ &\leq |N_0| + \frac{1}{\Gamma(q)}\lambda_0^*\alpha(r) + \frac{q\gamma t^{\gamma-1}B(q,\gamma)}{C(q)\Gamma(q)}\lambda_0^*\alpha(r) \\ &\leq |N_0| + \frac{1}{\Gamma(q)}\lambda_0^*\alpha(r) + \frac{q\gamma t^{\gamma-1}\Gamma(q)}{C(q)\Gamma(q)}\lambda_0^*\alpha(r)\end{aligned},$$

for $N \in Q_r$. Hence,

$$||MN||_Y \leq N_0 + \left\{\frac{1}{\Gamma(q)} + \frac{q\gamma t^{\gamma-1}\Gamma(q)}{C(q)\Gamma(q)}\right\}\lambda_0^*\alpha(r) < \infty. \tag{17}$$

As a result, on Y, M has uniform bounds. Now, let $t, u \in [0, T]$ such that $N \in Q_r$ and $t < u$. By indicating

$$sup_{t,N\in U\times Q_r}|W(t, N(t))| = W^* < \infty,$$

We estimate

$$\begin{aligned}&|M(N(u)) - M(N(t))|, \\ &\leq \left|\frac{q\gamma t^{\gamma-1}W(u, N(u))}{C(q)} - \frac{q\gamma t^{\gamma-1}W(t, N(t))}{C(q)}\right. \\ &\left.+\frac{1}{\Gamma(q)}\int_0^t (u-\xi)^{q-1}|W(\xi, N(\xi))|d\xi - \frac{1}{\Gamma(q)}\int_0^t (t-\xi)^{q-1}|W(t, N(t))|d\xi\right|, \\ &\leq \frac{q\gamma t^{\gamma-1}W^*}{C(q)}\left(u^{\gamma-1} - t^{\gamma-1}\right) + \frac{W^*}{\Gamma(q)}\left|\int_0^t (u-\xi)^{q-1}d\xi - \frac{1}{\Gamma(q)}\int_0^t (t-\xi)^{q-1}d\xi\right|, \\ &\leq \frac{q\gamma t^{\gamma-1}W^*}{C(q)}\left(u^{\gamma-1} - t^{\gamma-1}\right) + \frac{\gamma q W^* B(\gamma, q)}{\Gamma(q)\Gamma(\gamma+q)}\left(u^{\gamma+q-1} - t^{\gamma+q-1}\right), \\ &\leq \frac{q\gamma t^{\gamma-1}W^*}{C(q)}\left(u^{\gamma-1} - t^{\gamma-1}\right) + \frac{\gamma q W^* \Gamma(q)}{\Gamma(q)\Gamma(\gamma+q)}\left(u^{\gamma+q-1} - t^{\gamma+q-1}\right).\end{aligned} \tag{18}$$

As $u \to t$, we can observe that the right-hand (RH) side of Equation (18) approaches 0 independently of N. Thus,

$$||M(N(u)) - M(N(t))||_Y \to 0$$

as $u \to t$. The Arzela–Ascoli theorem uses this to determine the equicontinuity of M and, in turn, the compactness of M on Qr. Given the fulfillment of Theorem 1 on M, we have (A) or (B). We set from (B)

$$\Theta := \{N \in Y : \ ||N||_Y < \omega\},$$

for some $\omega > 0$, such that

$$N_0 + \left\{\frac{q\gamma T^{\gamma-1}}{\Gamma(q)} + \frac{q\gamma T^{\gamma-1}\Gamma(q)}{C(q)\Gamma(q)}\right\}\lambda_0^*\alpha(r) < \omega$$

From (C) and Equation (16), we have

$$||MN||_Y \leq N_0 + \left\{\frac{q\gamma T^{\gamma-1}}{\Gamma(q)} + \frac{q\gamma T^{\gamma-1}\Gamma(q)}{C(q)\Gamma(q)}\right\}\lambda_0^*\alpha(|N|_Y). \tag{19}$$

Assume that $N = \mu M(N)$ for all $N \in \partial\Theta$ and all $0 < \mu < 1$. Next, we write, using Equation (19),

$$\omega = ||N||_Y = \mu||MN||_Y < ||MN||_Y \leq N_0 + \left\{\frac{q\gamma T^{\gamma-1}}{\Gamma(q)} + \frac{q\gamma T^{\gamma-1}\Gamma(q)}{C(q)\Gamma(q)}\right\}\lambda_0^*\alpha(|N|_Y).$$
$$\leq N_0 + \left\{\frac{q\gamma T^{\gamma-1}}{\Gamma(q)} + \frac{q\gamma T^{\gamma-1}\Gamma(q)}{C(q)\Gamma(q)}\right\}\lambda_0^*\alpha(\omega) < \omega,$$

which is untrue. Therefore, by Theorem 1, Θ admits a fixed point in Θ and (B) is not satisfied. This demonstrates that the NFDFSCS (5) has an answer. □

3.2. Uniqueness of the NFDFSCS (5)

In order to demonstrate the originality of our approach to our issue, the NFDFSCS (5), we first investigate the Lipschitz property of the NFDFSCS (5).

Theorem 3. *Now, consider* $y_1, y_2, y_3, y_4,\ y_1^*, y_2^*, y_3^*, y_4^* \in C = C\ (J;\ R)$, *and consider*

A. $||y_1|| < \beta_1, ||y_2|| < \beta_2, ||y_3|| < \beta_3, ||y_4|| < \beta_4$ *for some constant* $\beta_1, \beta_2, \beta_3, \beta_4 > 0$.

Then, using constants $k_1,\ k_2,\ k_3,\ k_4$ *with regard to the pertinent components, W1, W3, W2, and W4, specified in the NFDFSCS (5), satisfy the Lipschitz property.*

Proof. Taking randomly $y_1; y_1^* A = A(U, R)$, for $W1$, we have

$$\begin{aligned}
&||W_1(t, N) - W_1(t, N^*)||,\\
&= ||(-ny_1) - (-ny_1^*)||,\\
&= || - ny_1 + ny_1^*||,\\
&\leq |n|||y_1 - y_1^*||,\\
&\leq \beta_1||y_1 - y_1^*||,
\end{aligned}$$

We determine that, with the constant $\beta_1 > 0$, W_1 is Lipschitz with regard to $y_1(t)$ based on the NFDFSCS (5).

Similarly, from the NFDFSCS (5), we find that all W_2, W_3, and W_4 are Lipschitz with regard to $y_2,\ y_3$, and y_4 under the constants $\beta_2,\ \beta_3,\ \beta_4 > 0$, respectively.

Therefore, the kernel functions W_1, W_2, W_3, and W_4 are Lipschitz, respectively, with constants $\beta_1, \beta_2,\ \beta_3,\ \beta_4 > 0$.

We now use Theorem 3 to show that the solution to the NFDFSCS (5) is unique. □

3.3. Stability of Ulam–Hyers

Ulam–Hyers stability originates from a problem posed by Stanisław Ulam in 1940, concerning the stability of functional equations [40]. Ulam's problem asked whether a function approximately satisfying a functional equation could be approximated by an exact solution. In 1941, Hyers provided a solution for Banach spaces, demonstrating that if a function $f : E_1 \to E_2$ (where E_1 and E_2 are Banach spaces) approximately satisfies the Cauchy functional equation $f(x + y) = f(x) + f(y)$, then there exists an exact additive function close to f. Specifically, for any $\in \geq 0$, if $|f(x + y) - f(x) - f(y)| \leq \in$ for all x, y, then there exists a unique additive function a such that $|f(x) - a(x)| \leq \in$ for all x [41].

The concept of Ulam–Hyers stability has been extended to various types of functional equations and different stability conditions, such as generalized Ulam–Hyers stability and Ulam–Hyers–Rassias stability. These extensions deal with different control functions and provide robustness against perturbations in equations. The applications of Ulam–Hyers stability are broad, including ensuring the stability of solutions in differential equations and control systems, providing a tool to analyze the robustness of mathematical models under small changes in system parameters. This stability concept is essential in ensuring that approximate solutions of functional equations can reliably be approximated by exact solutions, maintaining the integrity of mathematical and practical models.

The stability of the NFDFSCS (5) model solutions for four groups is examined in this section. We take into consideration four distinct concepts of stability in light of the need to provide solid mathematical underpinnings for the model. More specifically, we demonstrate stability regarding the Ulam–Hyers and Ulam–Hyers–Rassias concepts [41] and their corresponding generalizations for our NFDFSCS (5). Stability analysis plays a crucial role in guaranteeing the predictability and trustworthiness of mathematical models, particularly in practical applications like the system of chaotic SCM.

Theorem 4. *Assume that $N^*(t) \in Y$ is a solution of the NFDFSCS (5), for each $e_i > 0$, where $i = 1, 2, 3, 4$. Then, the functions $N^*(t) \in Y$ satisfy the inequalities listed below:*

$$\begin{aligned}\left|\Upsilon^*(t) - \left(\Upsilon_0 + \frac{\gamma(1-q)t^{\gamma-1}W_i(t,N(t))}{C(q)} + \frac{1}{\Gamma(q)}\int_0^t (t-\xi)^{q-1}W_i(\xi,N(\xi))d\xi\right)\right| \\ \leq \left[\frac{q\gamma T^{\gamma-1}}{\Gamma(q)} + \frac{q\gamma T^{\gamma-1}\Gamma(q)}{C(q)\Gamma(q)}\right]e_i\end{aligned} \tag{20}$$

Proof. Let us say that $e_i > 0$. Given that $N^*(t) \in Y$ fulfils

$$\begin{aligned}\left|{}^C D_t^q \Upsilon^*(t) - W_i(t, N^*(t))\right| < e_i, \\ {}^C D_t^q \Upsilon^*(t) = W_i(t, N^*(t)) + b_i(t),\end{aligned}$$

and $|b_i(t)| < e_i$. Clearly,

$$\Upsilon^*(t) = \Upsilon_0 + \frac{\gamma(1-q)t^{\gamma-1}[W_i(t,N(t)) + b_i(t)]}{C(q)} + \frac{1}{\Gamma(q)}\int_0^t (t-\xi)^{q-1}[W_i(\xi,N(\xi)) + b_i(t)]d\xi.$$

Here, we estimate

$$\begin{aligned}\left|\Upsilon^*(t) - \left(\Upsilon_0 + \frac{\gamma(1-q)t^{\gamma-1}W_i(t,N(t))}{C(q)} + \frac{1}{\Gamma(q)}\int_0^t (t-\xi)^{q-1}W_i(\xi,N(\xi))d\xi\right)\right| \\ \leq \left[\frac{q\gamma T^{\gamma-1}}{\Gamma(q)} + \frac{q\gamma T^{\gamma-1}\Gamma(q)}{C(q)\Gamma(q)}\right]e_i. \\ \leq \frac{\gamma(1-q)t^{\gamma-1}|b_i(t)|}{C(q)} + \frac{1}{\Gamma(q)}\int_0^t (t-\xi)^{q-1}|b_i(t)|d\xi. \\ \leq \frac{\gamma(1-q)t^{\gamma-1}e_i}{C(q)} + \frac{\Gamma(\gamma)}{\Gamma(q+\gamma)}e_i, \\ \leq \left\{\frac{\gamma(1-q)t^{\gamma-1}}{C(q)} + \frac{\Gamma(\gamma)}{\Gamma(q+\gamma)}\right\}e_i,\end{aligned} \quad , \tag{21}$$

This indicates that Equation (19) is met. Similarly, we prove the NFDFSCS (5). □

4. Boundedness of the NFDFSCS (5)

In this section, we will estimate the global Mittag-Leffler attractive set (MLAS) and Mittag-Leffler positive invariant set (MLPIS) for the proposed system.

Lemma 1 ([38]). Let $f(t) \in R$ be a smooth function; then, ${}^C_{t_0}D_t^q(f^2(t)) \leq 2f(t){}^C_{t_0}D_t^q(f(t))$, $t \geq t_0$, $0 < q < 1$.

Lemma 2 ([38]). Let $q \in (0,1)$ and a constant $\Xi \in R$. If a continuous function $f(t)$ satisfies ${}^C_{t_0}D_t^q(f(t)) \leq \Xi f(t)$, then $f(t) \leq f(0)E_q(\Xi t^q)$, for the case of $t \geq 0$.

Theorem 5. *Let $n > 0$, $c > 0$, $k < 1$, $\varpi > 0$, $\mu > 0$, and the global MLAS and MLPIS of the system are as follows:*

$$\Psi_{\varpi,\mu} = \left\{ y(t) \in R^4 \middle| c\varpi y_1^2 + \varpi y_2^2 + \mu y_3^2 + \mu \left(y_4 - \frac{\varpi m + \mu r}{\mu} \right)^2 \leq T_{1\max}^2 \right\},$$

where

$$T_{1\max}^2 = \frac{(\varpi m + \mu r)^2 (1-k)}{\mu \eta}, \eta = \min\{n, n+1, 1, 1-k\} > 0.$$

Define the following generalized positively definite and radically unbounded Lyapunov function:

$$V_{\varpi,\mu}(y_1, y_2, y_3, y_4) = \frac{1}{2} c\varpi y_1^2 + \frac{1}{2} \varpi y_2^2 + \frac{1}{2} \mu y_3^2 + \frac{1}{2} \mu \left(y_4 - \frac{\varpi m + \mu r}{\mu} \right)^2,$$

where $\varpi > 0$, $\mu > 0$, $c > 0$. By applying the fractional derivative to $V_{\varpi,\mu}$ and using Lemma 1, we can obtain

$$D_t^q V_{\varpi,\mu}(y(t)) \leq \varpi c y_1 D_t^q y_1 + \varpi y_2 D_t^q y_2 + \mu D_t^q y_3 + \mu (y_4 - \frac{\varpi m + \mu r}{\mu}) D_t^q y_4$$

$$= -\frac{1}{2} n\varpi c y_1^2 - \frac{1}{2} \varpi (n+1) y_2^2 - \frac{1}{2} \mu y_3^2 - \frac{1}{2} \mu (1-k) \left(y_4 - \frac{\varpi m + \mu r}{\mu} \right)^2 + F(y(t)),$$

where

$$F(y(t)) = -\frac{1}{2} n\varpi c y_1^2 - \frac{1}{2} \varpi (n+1) y_2^2 - \frac{1}{2} \mu y_3^2 - \frac{1}{2} \mu (1-k) y_4^2 + \frac{1}{2} \frac{(\varpi m + \mu r)^2 (1-k)}{\mu}. \quad (22)$$

It is obvious that $F(y(t)) \leq \sup F(y(t)) = l_{\varpi,\mu} = \frac{1}{2} \frac{(\varpi m + \mu r)^2 (1-k)}{\mu}$, and we have

$$D_t^q V_{\varpi,\mu}(y(t)) \leq -\eta V_{\varpi,\mu} + l_{\varpi,\mu}, \quad (23)$$

$$D_t^q (V_{\varpi,\mu}(t) - \frac{l_{\varpi,\mu}}{\eta}) \leq -\eta (V_{\varpi,\mu} - \frac{l_{\varpi,\mu}}{\eta}). \quad (24)$$

According to Lemma 2, we have

$$V_{\varpi,\mu}(t) - \frac{l_{\varpi,\mu}}{\eta} \leq (V_{\varpi,\mu}(0) - \frac{l_{\varpi,\mu}}{\eta}) E_q(-\eta t^q), t \geq 0. \quad (25)$$

Based on Definition 3, we can conclude that $\Psi_{\varpi,\mu}$ with $n > 0$, $c > 0$, $k < 1$, $\varpi > 0$, $\mu > 0$ is the MLAS and MLPIS for the system. If we take $q = 0.98$, $n = 0.2$, $m = 3.6$, $r = 27$, $k = 0.1$, $c = 0.6$, $\varpi = 1$, $\mu = 1$, then $\Psi = \left\{ y(t) \in R^4 \middle| 0.6y_1^2 + y_2^2 + (y_3 - 30.6)^2 \leq (64.91)^2 \right\}$, and Figure 2 *shows the phase portraits and MLAS of system (5).*

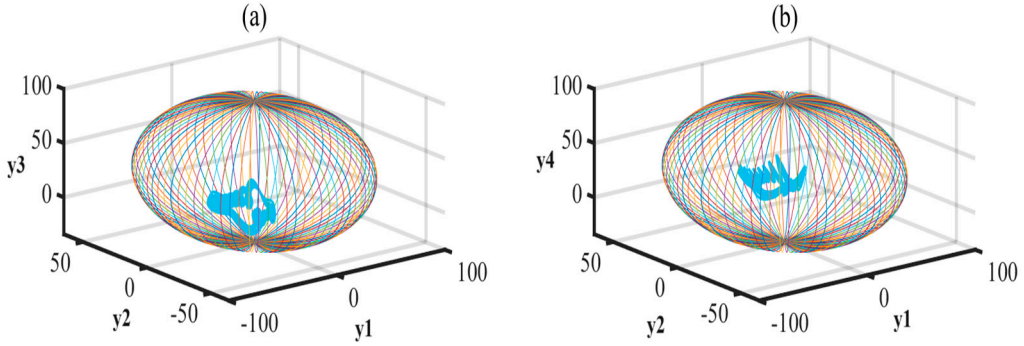

Figure 2. *Cont.*

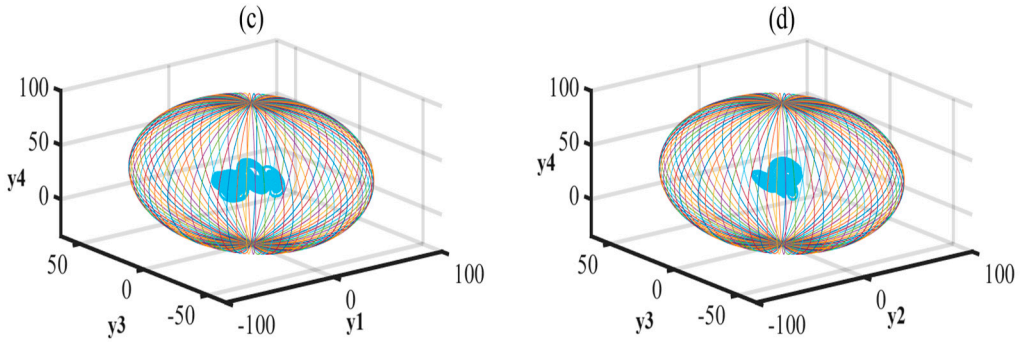

Figure 2. The phase portraits and boundedness of system (5), where $q = 0.98$, $n = 0.2$, $m = 3.6$, $r = 27, k = 0.1, c = 0.6, p = 0.2$: (**a**) y_1-y_2-y_3 plane, (**b**) y_1-y_2-y_4 plane, (**c**) y_1-y_3-y_4 plane, and (**d**) y_2-y_3-y_4 plane.

5. Numerical Simulation

The following Cauchy problem is discussed in this section.

$$ {}_0^C D_t^q y(t) = g(t, y(t)) $$

$$ y(0) = y_0 $$

The new fractal fractional derivative is contained in the differential operator. We modify the previous equation using a new integral with a power-law kernel.

$$ y(t) = \frac{1}{\Gamma(q)} \int_0^t g(\tau, y(\tau))(t-\tau)^{q-1} \tau^{1-\beta} d\tau $$

At the point $t_{\delta+1} = (\delta+1)\Delta t$,

$$ y(t_{\delta+1}) = \frac{1}{\Gamma(q)} \int_0^{t_{\delta+1}} G(\tau, y(\tau))(t_{\delta+1}-\tau)^{q-1} d\tau $$

where

$$ G(\tau, y(\tau)) = g(\tau, y(\tau))\tau^{1-\beta} $$

Then, we have

$$ y(t_{\delta+1}) = \frac{1}{\Gamma(q)} \sum_{\mu=2}^{\delta} \int_{t_\delta}^{t_{\delta+1}} G(\tau, y(\tau))(t_{\delta+1}-\tau)^{q-1} d\tau $$

We obtain the following when we place the Newton polynomial in the equation above.

$$ \begin{aligned} y^{\delta+1} &= \frac{1}{\Gamma(q)} \sum_{\mu=2}^{\delta} G\left(t_{\mu-2}, y^{\mu-2}\right)\Delta t \int_{t_\delta}^{t_{\delta+1}} (t_{\delta+1}-\tau)^{q-1} d\tau \\ &+ \frac{1}{\Gamma(q)} \sum_{\mu=2}^{\delta} \frac{G\left(t_{\mu-1}, y^{\mu-1}\right) - G\left(t_{\mu-2}, y^{\mu-2}\right)}{\Delta t} \\ &\times \int_{t_\delta}^{t_{\delta+1}} \left(\tau - t_{\mu-2}\right)(t_{\delta+1}-\tau)^{q-1} d\tau \\ &+ \frac{1}{\Gamma(q)} \sum_{\mu=2}^{\delta} \frac{G\left(t_\mu, y^{\mu}\right) - 2G\left(t_{\mu-1}, y^{\mu-1}\right) + G\left(t_{\mu-2}, y^{\mu-2}\right)}{2(\Delta t)^2} \\ &\times \int_{t_\delta}^{t_{\delta+1}} \left(\tau - t_{\mu-2}\right)\left(\tau - t_{\mu-1}\right)(t_{\delta+1}-\tau)^{q-1} d\tau \end{aligned} $$

We use $G(t, y(t)) = t^{1-\beta} g(t, y(t))$. The following scheme can be generated from the previous equation:

$$
\begin{aligned}
y^{\delta+1} &= \frac{(\Delta t)^{\alpha}}{\Gamma(q+1)} \sum_{\mu=2}^{\delta} t_{\mu-2}^{1-\beta} g\left(t_{\mu-2}, y^{\mu-2}\right) \\
&\times \left[(\delta-\mu+1)^{q} - (\delta-\mu)^{q}\right] \\
&+ \frac{(\Delta t)^{q}}{\Gamma(q+2)} \sum_{\mu=2}^{\delta} \begin{bmatrix} t_{\mu-1}^{1-\beta} g\left(t_{\mu-1}, y^{\mu-1}\right) \\ -t_{\mu-2}^{1-\beta} g\left(t_{\mu-2}, y^{\mu-2}\right) \end{bmatrix} \\
&\times \begin{bmatrix} (\delta-\mu+1)^{q}(\delta-\mu+3+2q) \\ -(\delta-\mu)^{q}(\delta-\mu+3+3q) \end{bmatrix} \\
&+ \frac{(\Delta t)^{q}}{2\Gamma(q+3)} \sum_{\mu=2}^{\delta} \begin{bmatrix} t_{\mu}^{1-\beta} g\left(t_{\mu}, y^{\mu}\right) \\ -2t_{\mu-1}^{1-\beta} g\left(t_{\mu-1}, y^{\mu-1}\right) \\ +t_{\mu-2}^{1-\beta} g\left(t_{\mu-2}, y^{\mu-2}\right) \end{bmatrix} \\
&\times \begin{bmatrix} (\delta-\mu+1)^{q}\begin{bmatrix} 2(\delta-\mu)^{2} + (3q+10)(\delta-\mu) \\ +2q^{2}+9q+12 \end{bmatrix} \\ -(\delta-\mu)^{q}\begin{bmatrix} 2(\delta-\mu)^{2} + (5q+10)(\delta-\mu) \\ +6q^{2}+18q+12 \end{bmatrix} \end{bmatrix}
\end{aligned}
$$

The mathematical analysis of a chaotic supply chain model incorporating a non-linear incidence has been presented. Advanced techniques have been employed to derive theoretical outcomes and assess their efficacy. Fascinating discoveries have been made through the application of non-integer parametric values in the chaotic supply chain model. y_1 comprises individuals at risk of chaotic supply chain model exposure, while y_2, y_3, and y_3 represent those currently affected. The convergence solution for endemic and disease-free equilibria using the power-law scheme at $h = 0.1$ is shown in the figure. The employed technique has demonstrated a positive impact in terms of controlling the chaotic supply chain model, as shown in Figures 3 and 4.

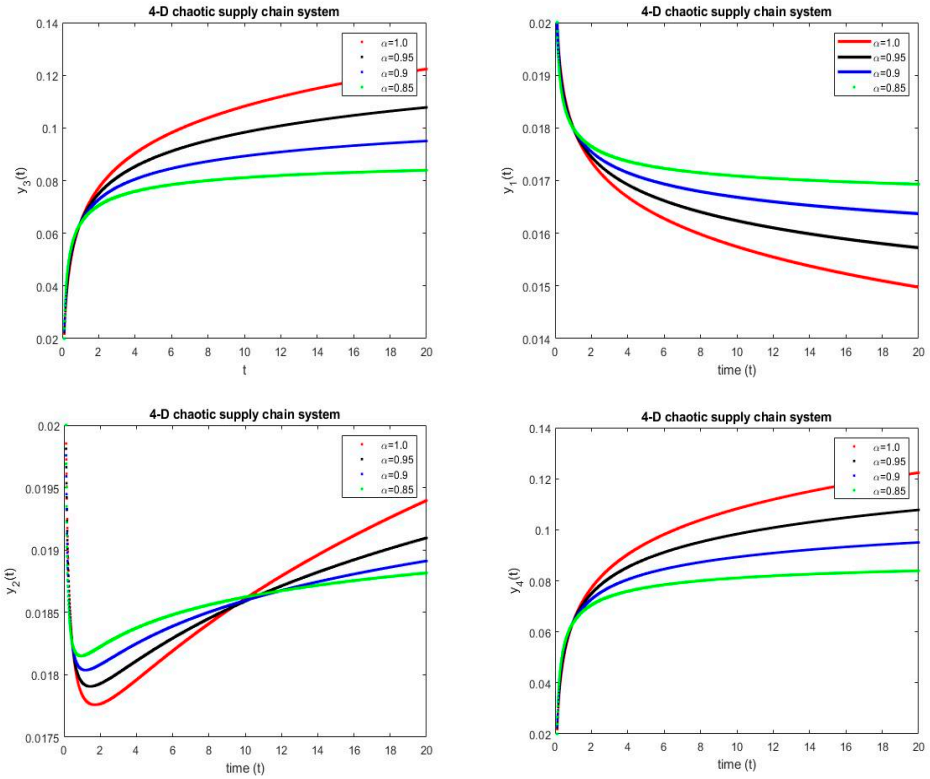

Figure 3. Simulation of compartments with proposed fractional-order scheme at dimension 0.9.

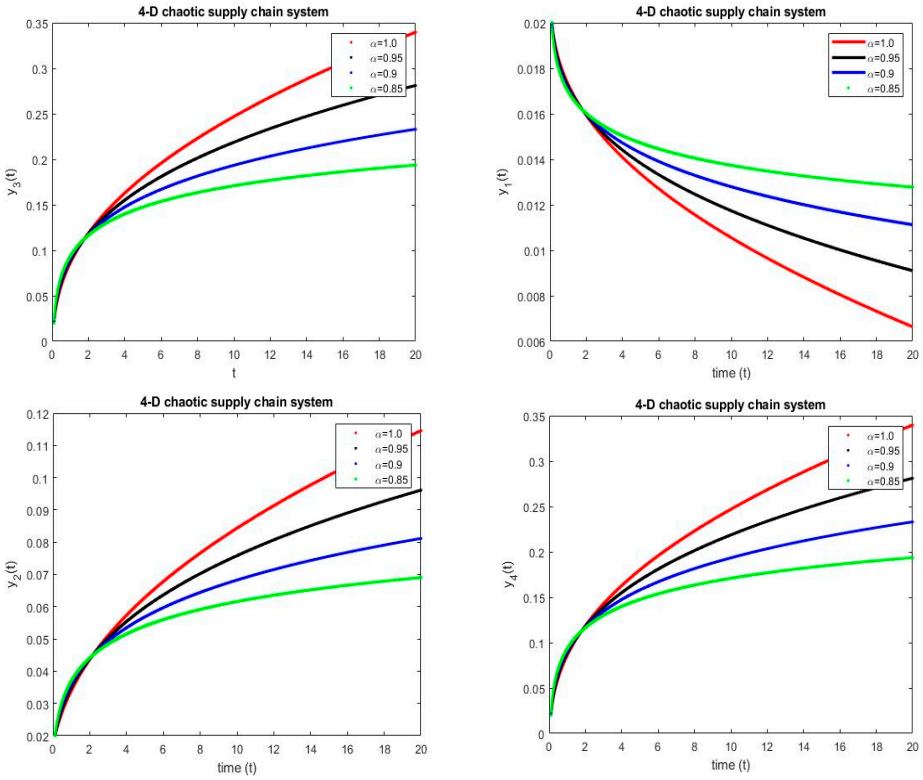

Figure 4. Simulation of compartments with proposed fractional-order scheme at dimension 1.

By using the abovementioned techniques that use a power-law kernel, we obtain the numerical simulation, and the graphs demonstrate the numerical simulation results for the different values of $q = 0.95,\ 0.90,\ 0.85,\ 1.0$. Initially (Figures 3 and 4), we can see that, in all cases, as the fractional-order derivative grows, the y_1 compartment decreases, while y_2 grows as the fractional-order value grows. It effectively lowers the y_1 rate while increasing the populations of all y_2, y_3, and y_4.

6. Dynamical Analysis

Case 1: Let $\{m, n, r, k, p\} = \{3.6, 2, 27, 0.3, 0.2\}$ and c varies.

Let m, n, r, k, p be held constant at $3.6, 2, 27, 0.3, 0.2$, respectively, while c is systematically varied within the range of 6 to 12. The bifurcation diagram of the system and the maximum Lyapunov exponent under these conditions are depicted in Figure 5a and Figure 5b, respectively.

When $c \in (8.8, 9.1) \cup (10.4, 10.6) \cup (11.4, 11.9)$, the system is periodic and it is chaotic with the MLE increasing when $c \in (6, 8.8) \cup (9.1, 10.4) \cup (10.6, 11.4) \cup (11.9, 12)$. The complexity diagrams depicted in Figure 5c are consistent with these results.

For some values of c, the phase portraits and the $p - s$ dynamics of the $0 - 1$ testing are given in Figure 6. System (3) is said to be periodic when $c = 0.9$ and $c = 11.81$, whereas it is chaotic when $c = 6.5$.

When c is set within certain ranges, the model exhibits chaotic dynamics. This chaotic behavior indicates a high degree of unpredictability and variability in the system's response to changes in the demand and supply conditions. In practical terms, when c induces chaos, the supply chain system becomes highly sensitive to fluctuations in the market conditions or disruptions, leading to significant variability in the inventory levels and order quantities. Moreover, in a supply chain context, periodic behavior induced by the contingency reserve coefficient suggests a more predictable and regular pattern of inventory levels and order quantities, corresponding to stable market conditions where the demand and supply follow a cyclical pattern.

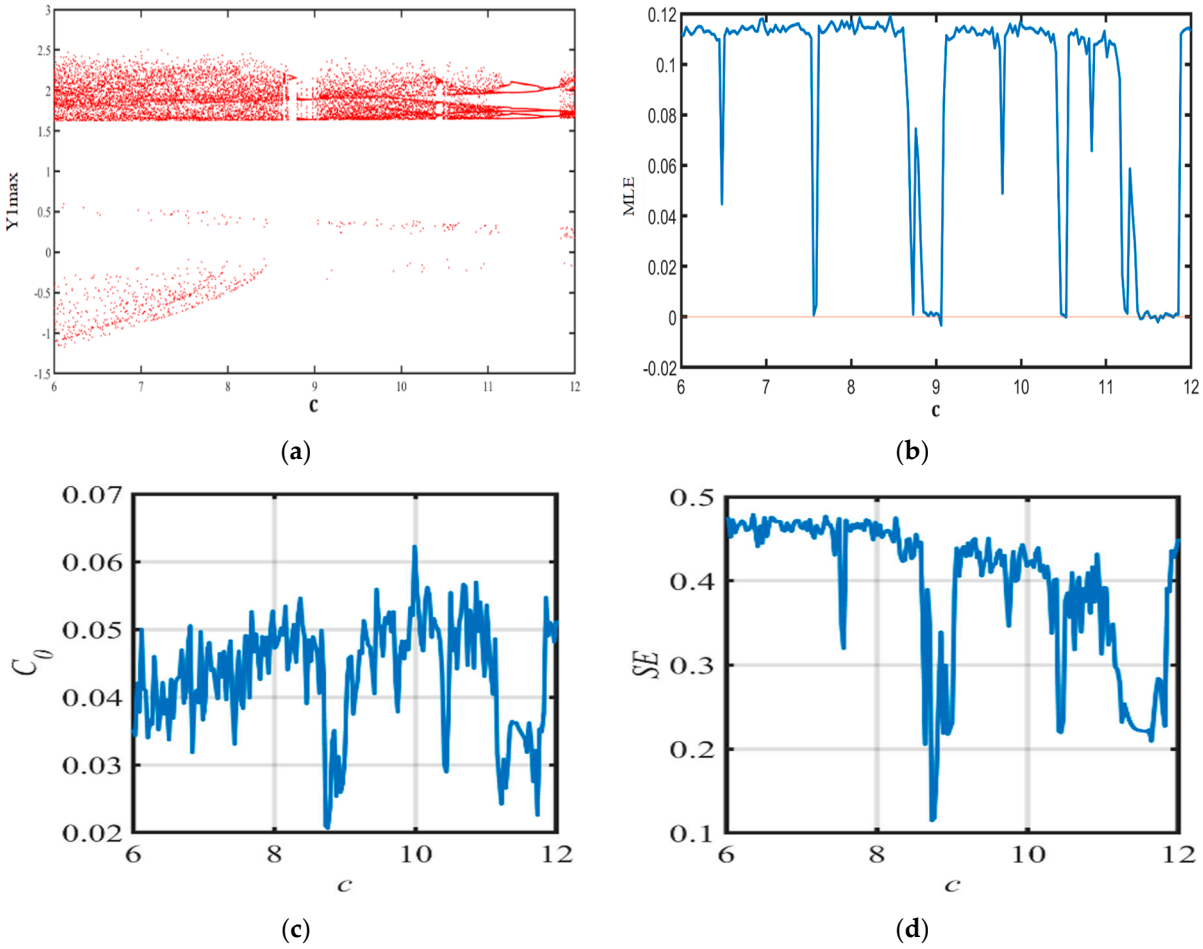

Figure 5. MATLAB simulation of the 4DCSC system (3) with c when $m = 3.6$, $n = 2$, $r = 27$, $k = 0.3$, $p = 0.2$: (**a**) bifurcation diagram, (**b**) MLE graph, (**c**) C_0 analysis, and (**d**) complexity analysis.

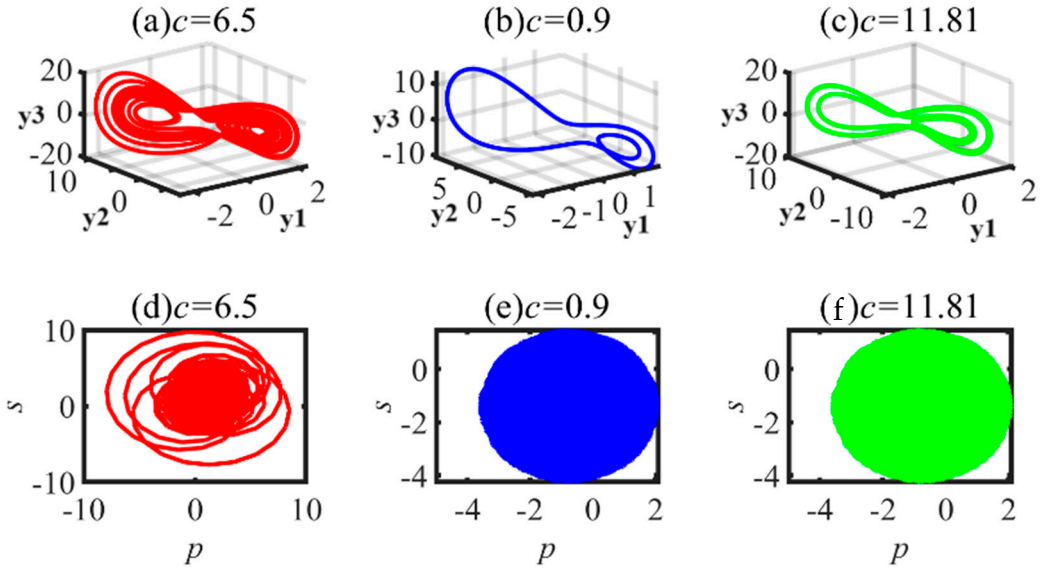

Figure 6. Phase portraits and p–s plots of 0–1 test for system when $m = 3.6$, $n = 2$, $r = 27$, $k = 0.3$, $p = 0.2$.

Case 2: Let $\{c, n, r, k, p\} = \{1.6, 2, 27, 0.3, 0.2\}$ and m varies.

To explore the behavior of the proposed model versus m, we maintain c, n, r, k and p is held constant at $1.6, 2, 27, 0.3, 0.2$, respectively, while m is systematically varied within

the range of 16 to 22. The bifurcation diagram of the system and the maximum Lyapunov exponent under these conditions are depicted in Figures 7a and 7b, respectively. The results indicate that the system shows inverse period-doubling bifurcation, and, as the parameter m decreases, the system moves from a periodic state, after the period-doubling bifurcation, to a chaotic state.

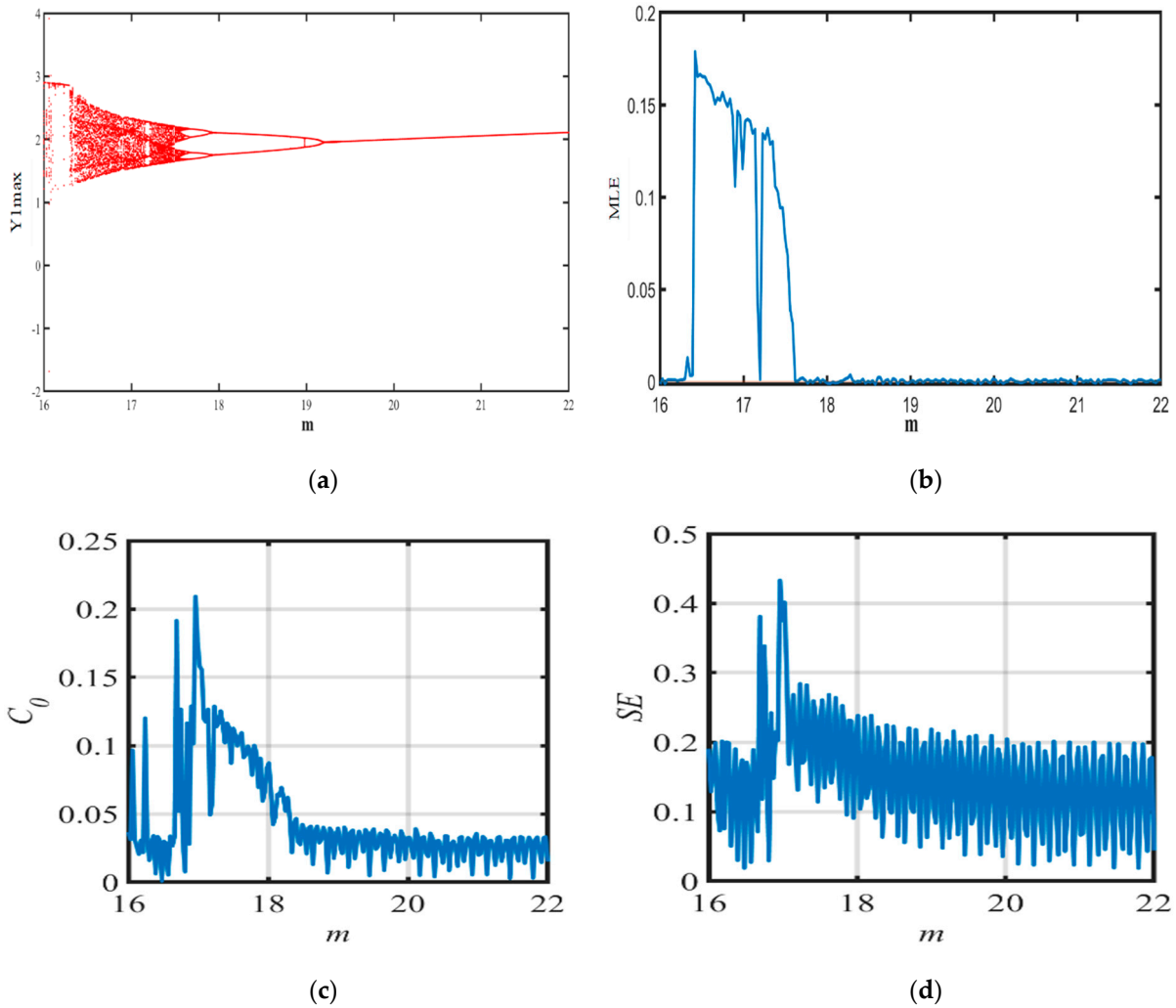

Figure 7. MATLAB simulation of 4DCSC system (3) with m when $c = 1.6$, $n = 2$, $r = 27$, $k = 0.3$, $p = 0.2$: (**a**) bifurcation diagram, (**b**) MLE graph, (**c**) C_0 analysis, and (**d**) complexity analysis.

When the value m lies in the range of $[19.2, 22]$, period one appears, and period-doubling bifurcation occurs for $m = 19.3$. When the value m lies in the range of $[17.8, 19.2]$, period two appears. Then, period four appears within the range of $[17.5, 17.8]$. Meanwhile, when the value of m lies in the range of $[16, 17.5]$, the behavior of the system becomes chaotic. These results are also consistent with the complexity diagrams depicted in Figure 7c.

For some values of m, Figure 8 shows the phase portraits as well as the $p - s$ dynamics of the 0–1 testing. It appears that system is periodic when $m = 18.2$ and $m = 21$ and chaotic when $m = 16.7$.

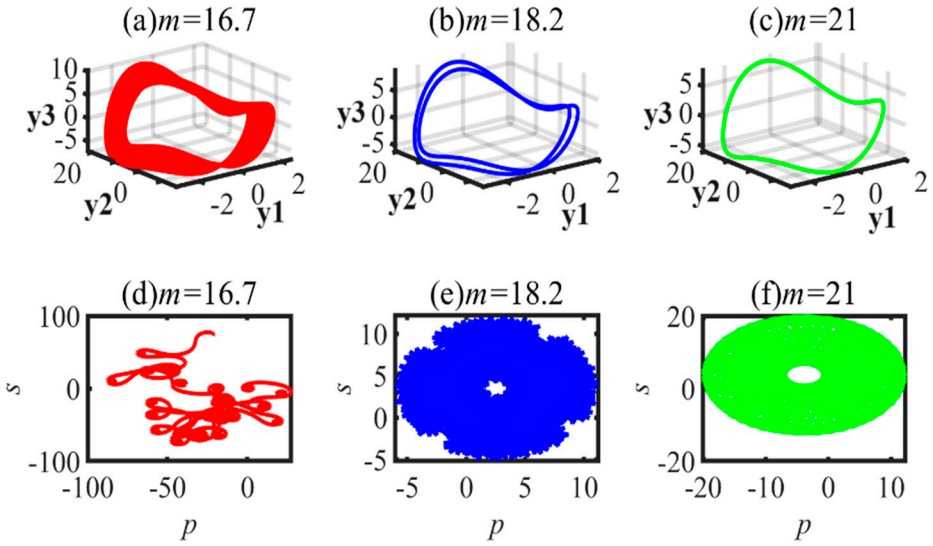

Figure 8. Phase portraits and p–s plots of 0–1 test for system when c = 1.6, n = 2, r = 27, k = 0.3, p = 0.2.

Chaotic behavior in the delivery efficiency of the distributor indicates a high degree of unpredictability and variability in the system's response to changes in delivery efficiency. This suggests that when m induces chaos, the supply chain system becomes highly sensitive to variations in the delivery performance, leading to significant fluctuations in the inventory levels and order quantities. In addition, the periodic behavior induced by the delivery efficiency of the distributor suggests a more predictable and regular pattern of inventory levels and order quantities, corresponding to consistent delivery performance by the distributor. Such periodicity can be advantageous for planning and forecasting, as it allows for more accurate predictions and efficient resource allocation.

Case 3: Let $\{c, m, n, r, k, p\} = \{1.6, 3.6, 2, 27, 0.3, 0.2\}$ and q varies.

In the NFDFSCS (5), let $\{c, m, n, r, k, p\} = \{1.6, 3.6, 2, 27, 0.3, 0.2\}$ and the parameter q is chosen as the critical variable to show the effect of the fractional order to the behavior of the chaotic system results. Figure 9a,b, respectively, depict the bifurcation diagram and maximum Lyapunov exponent. When $q \in (0.6, 0.63)$, the system is mostly in a stable state. When $q \in (0.63, 1)$, chaos appears and the system appears in a chaotic state.

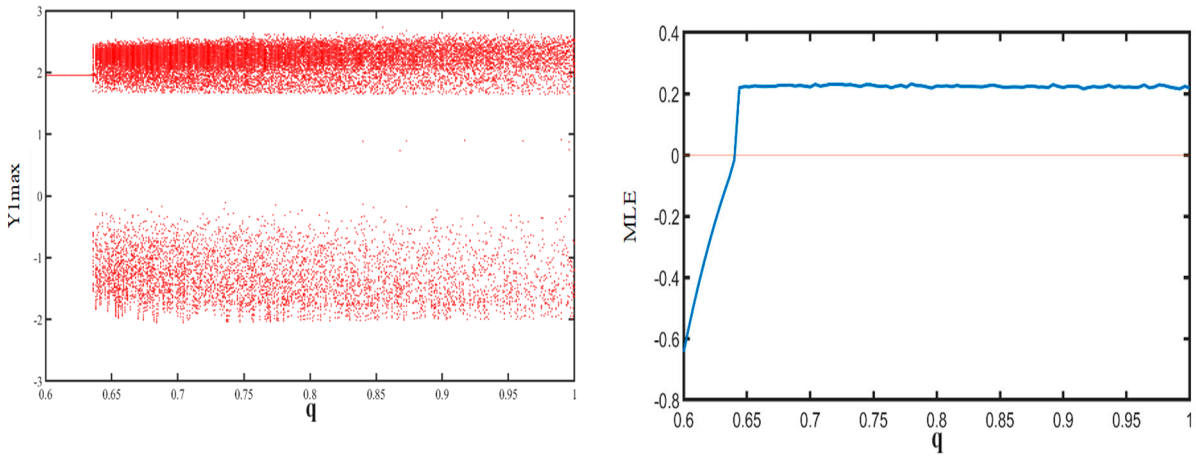

(**a**) (**b**)

Figure 9. *Cont.*

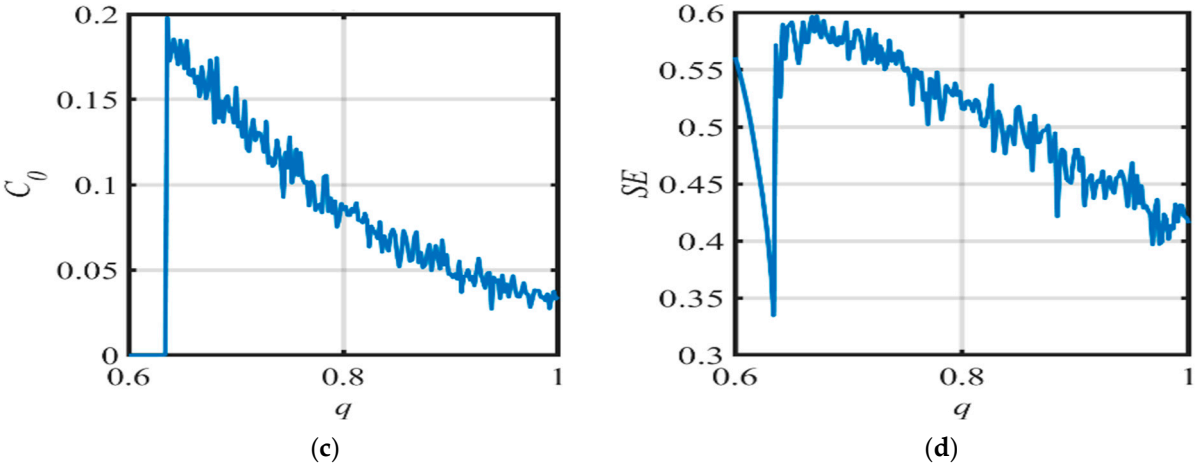

Figure 9. MATLAB simulation of the 4DCSC system (3) with q when m = 3.6, c = 1.6, n = 2, r = 27, k = 0.3, p = 0.2. (**a**) Bifurcation diagram, (**b**) MLE graph, (**c**) C_0 analysis, and (**d**) complexity analysis.

As shown in Figure 9c,d, the C_0 complexity and SE complexity of the system are lower when $q \in (0.6, 0.63)$, and the values of the complexity both oscillate at higher values when $q \in (0.63, 1)$. We find that the complexity results are consistent with the bifurcation diagrams, indicating that the complexity can reflect the dynamic characteristics of the proposed system.

For some values of q, the phase portraits and the p–s dynamics of the 0–1 testing are given in Figure 10. The system is stable for q = 0.63, while being chaotic when $q = 0.8$ and $q = 0.95$. This means that the system becomes chaotic with fractional order q rising.

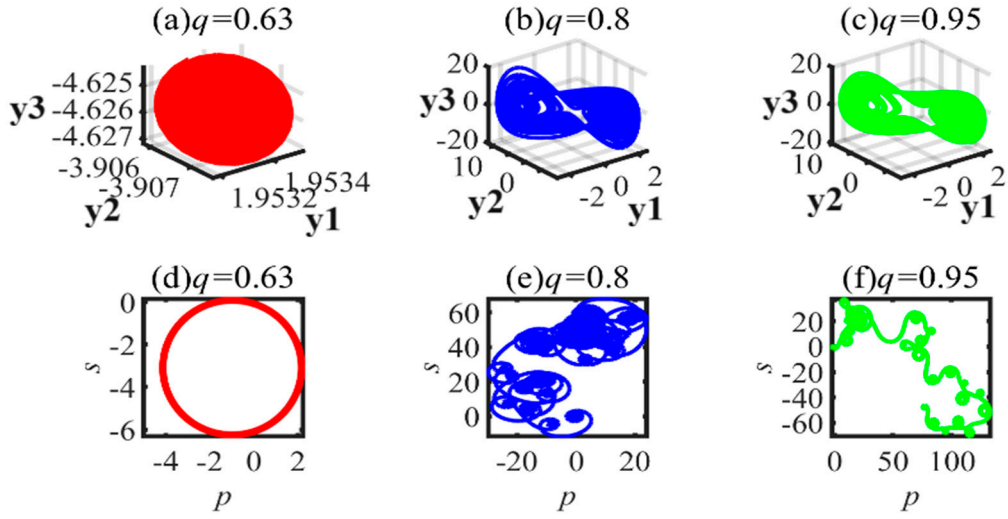

Figure 10. Phase portraits and p–s plots of 0–1 test for system when m = 3.6, c = 1.6, n = 2, r = 27, k = 0.3, p = 0.2.

In the proposed 4D Chaotic Supply Chain Model (4DCSCM), the fractional-order parameter q significantly influences the system's dynamic behavior. This parameter is associated with the memory effect and hereditary properties of the system, reflecting the long-term dependencies between various supply chain components. A fractional order q leading to chaos indicates that the supply chain system's current state is heavily influenced by its past states, resulting in a highly unpredictable and variable response to changes in demand, supply, and other factors. Moreover, a fractional order q leading to periodic behavior indicates that the memory effect and hereditary properties, as captured by the fractional order q, lead to more predictable and stable dynamics within the supply chain.

Periodicity in this context means that past states have a consistent and regular influence on future states, resulting in a stable cycle of inventory levels and order quantities. This predictability allows supply chain managers to optimize their operations by relying on regular patterns for planning and forecasting, thus enhancing the efficiency of inventory management, reducing the costs, and improving the service levels.

7. Finite-Time Stabilization of System

Finite-time stabilization refers to the control process whereby the system's state is driven to an equilibrium point in a finite period of time. Unlike asymptotic stabilization, which ensures that the system's state approaches equilibrium as time progresses to infinity, FTS guarantees that the state will reach equilibrium within a specified finite time. This concept is particularly useful in applications requiring quick system responses and precise control actions. The advantage of FTS lies in its ability to ensure rapid convergence and improved robustness against disturbances and uncertainties in the system [42].

The methodology of finite-time stabilization often employs Lyapunov functions and control laws specifically designed to achieve the desired stabilization within a finite duration. The theoretical underpinnings of FTS are rooted in the mathematical analysis of dynamical systems and control theory, offering a framework for the design of controllers that can achieve rapid stabilization. This approach has been widely applied in various fields, including robotics, aerospace, and networked systems, where the speed of response and reliability are critical.

In this section, we design an effective control scheme to stabilize the model in a finite time. The controlled fractional order system is given as

$$\begin{cases} D_t^q y_1 = -(y_2 + n y_1) + u_1 \\ D_t^q y_2 = m y_3 - (n+1) y_2 - p y_1 y_3 + c y_1 + u_2 \\ D_t^q y_3 = r y_2 - y_3 - y_2 y_4 + u_3 \\ D_t^q y_4 = -(1-k) y_4 + y_2 y_3 + u_4 \end{cases} \tag{26}$$

where u_1, u_2, u_3, u_4 are the control parameters of the system. Now, the control goal is to design a suitable robust controller to stabilize the system around zero in a finite time.

Lemma 3 ([43]). *Assume that $\Omega \subset R^n$ is a domain containing the origin and $V(t, Y)$ is a continuously differentiable function and locally Lipschitz, so that*

$$\gamma_1(\|Y\|^a) \leq V(t, Y) \leq \gamma_2(\|Y\|^{ab}), D_t^q V(t, Y) \leq \gamma_3(\|Y\|^{ab})$$

where $0 < q < 1, a > 0, b > 0, \gamma_i > 0 (i = 1, 2, 3)$; then, the system is called Mittag-Leffler stable.

Theorem 6. *The controlled chaotic system can be finite-time stabilized by the controller,*

$$\begin{cases} u_1 = n y_1 + y_2 - \frac{k}{2} y_1^s \\ u_2 = (n+1) y_2 - c y_1 - m y_3 + p y_1 y_3 - \frac{k}{2} y_2^s \\ u_3 = y_3 - r y_2 - \frac{k}{2} y_3^s \\ u_4 = (1-k) y_4 - \frac{k}{2} y_4^s \end{cases},$$

where $0 < s < 1, k > 0$, and the finite time T is estimated by

$$T \leq \left[(y_1^2 + \ldots + y_4^2)^{q - \frac{1+s}{2}} (0, Y) \frac{\Gamma(1 - \frac{1+s}{2}) \Gamma(1+q)}{k \Gamma(q - \frac{1+s}{2} + 1)} \right]^{\frac{1}{q}}.$$

Proof. To prove the stability of the system, let us use the classic Lyapunov direct method and define the following Lyapunov function:

$$V(T,Y) = y_1^2 + y_2^2 + y_3^2 + y_4^2.$$

Calculating the fractional derivative of the Lyapunov function and using Lemma 3, one can obtain

$$\begin{aligned} D_t^q V(T,Y) &\leq 2y_1 D_t^q y_1 + 2y_2 D_t^q y_2 + 2y_3 D_t^q y_3 + 2y_4 D_t^q y_4 \\ &= 2y_1(-y_2 - ny_1 + u_1) + 2y_2(my_3 - (n+1)y_2 - py_1y_3 + cy_1 + u_2) \\ &+2y_3(ry_2 - y_3 - y_2y_4 + u_3) + 2y_4(-y_4 + ky_4 + y_2y_3 + u_4) \\ &= -ky_1^{1+s} - ky_2^{1+s} - ky_3^{1+s} - ky_4^{1+s} \end{aligned}.$$

Then,

$$D_t^q(y_1^2 + \ldots y_4^2) \leq -k(y_1^2 + \ldots y_4^2)^{\frac{1+s}{2}}.$$

It is obvious that the Lyapunov function satisfies the conditions in Theorem 6. Thus, the system is Mittag-Leffler stable. □

We have

$$D_t^q(y_1^2 + \ldots y_4^2)^{q-\frac{1+s}{2}} = \frac{\Gamma(q - \frac{1+s}{2} + 1)}{\Gamma(1 - \frac{1+s}{2})}(y_1^2 + \ldots y_4^2)^{-\frac{1+s}{2}} D_t^q(y_1^2 + \ldots y_4^2),$$

Therefore,

$$D_t^q(y_1^2 + \ldots y_4^2)^{q-\frac{1+s}{2}} \leq -k\frac{\Gamma(q - \frac{1+s}{2} + 1)}{\Gamma(1 - \frac{1+s}{2})},$$

and one may take the integral of both sides from 0 to T as follows:

$$(y_1^2 + \ldots + y_4^2)^{q-\frac{1+s}{2}}(T,Y) - (y_1^2 + \ldots + y_4^2)^{q-\frac{1+s}{2}}(0,Y) \leq -k\frac{\Gamma(q - \frac{1+s}{2} + 1)}{\Gamma(1 - \frac{1+s}{2}\Gamma(1+q)}T^q.$$

The time is expressed as

$$T \leq \left[(y_1^2 + \ldots + y_4^2)^{q-\frac{1+s}{2}}(0,Y)\frac{\Gamma(1 - \frac{1+s}{2})\Gamma(1+q)}{k\Gamma(q - \frac{1+s}{2} + 1)}\right]^{\frac{1}{q}}.$$

The states of the system under the controller are depicted in Figure 11, which indicates that the trajectories of the system can be stabilized to the origin in a finite time. In addition, the chaotic behavior is suppressed. The numerical results show that changing α and k causes the system to converge to zero slowly.

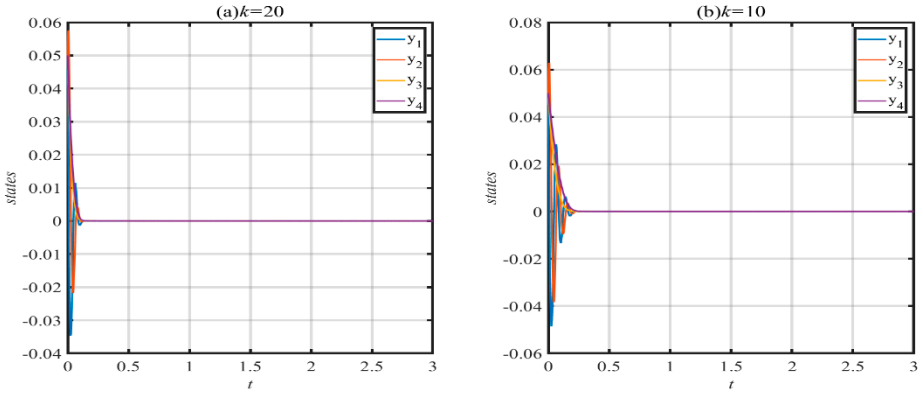

Figure 11. State trajectories of the controlled system with $q = 0.98$, $k = 20$, and $k = 10$.

A robust control scheme is designed to stabilize the system in a finite time, effectively suppressing chaotic behaviors. The numerical results demonstrate that the control strategy is effective in driving the system's state to an equilibrium point within a specified finite duration. This rapid stabilization is crucial for practical applications in supply chain management, where quick response times are essential.

8. Conclusions

This research examines the complex dynamics of an NFDFSCS that incorporates a quadratic interaction term between the customer demand and distributor inventory levels. Building on Xu et al. (2022) [35], this model enhances the chaotic behavior and complexity, indicated by the significantly larger MLE. The system's existence, uniqueness, and Ulam–Hyers stability are verified. Additionally, the study establishes global Mittag-Leffler attractive and positive invariant sets. Numerical simulations and MATLAB phase portraits confirm the system's chaotic nature, supported by Lyapunov exponents, bifurcation diagrams, 0–1 tests, and a complexity analysis. We have examined a mathematical model comprising a set of equations that elucidates the dynamics of the chaotic supply chain model. The investigation of this model has been extensively conducted and it has been determined that the system exhibits both local and global stability. A new numerical technique for newly created fractional differentiation is provided in this paper. The suggested Caputo fractional derivative scheme with a power law was investigated for the chaotic supply chain model in this research. Fixed point theory and an iterative approach were used to prove the existence and uniqueness of the system of solutions for the model. We obtained very effective results for the proposed model. A novel numerical approximation for the solution of non-linear fractional differential equations derived from this form of derivative was proposed within the context of fractional differentiation with a non-singular and non-local kernel. Additionally, the main result and the combined impact of infected external and internal parts of the body were illustrated in some numerical simulations, from which one can see that external and internal infections can both speed up. We discussed some theoretical conclusions regarding the model and demonstrated the efficacy of the strategies presented. Our findings will be extremely useful to those researching fractional derivative models.

Author Contributions: Conceptualization, A.S. and S.V.; methodology, M.D.J.; software, M.F., S.Z. and S.V.; validation, B.F., M.H. and M.D.J.; formal analysis, A.S. and S.Z.; investigation, M.F.; data curation, B.F. and M.H.; writing—original draft preparation, S.V., S.Z. and M.F.; writing—review and editing, A.S., M.D.J. and S.Z.; visualization, M.F. and S.V.; supervision, M.D.J.; funding acquisition, M.D.J. and S.Z. All authors have read and agreed to the published version of the manuscript.

Funding: This research was funded by Universitas Padjadjaran, providing the project's financial support. Moreover, Song Zheng thanks the First Class Discipline of Zhejiang-A (Zhejiang University of Finance and Economics-Statistics) and the Collaborative Innovation Center for Data Science and Big Data Analysis (Zhejiang University of Finance and Economics-Statistics).

Data Availability Statement: The data that support the findings of this study are available from the corresponding author on reasonable request.

Acknowledgments: We appreciate the comprehensive feedback and constructive recommendations provided by the peer reviewers, which markedly improved the overall quality and clarity of the manuscript.

Conflicts of Interest: The authors declare no conflict of interest.

References

1. Wang, H.; Weng, C.; Song, Z.; Cai, J. Research on the law of spatial fractional calculus diffusion equation in the evolution of chaotic economic system. *Chaos Solitons Fractals* **2020**, *131*, 109462. [CrossRef]
2. Sene, N. Introduction to the fractional-order chaotic system under fractional operator in Caputo sense. *Alex. Eng. J.* **2021**, *60*, 3997–4014. [CrossRef]

3. He, S.; Wang, H.; Sun, K. Solutions and memory effect of fractional-order chaotic system: A review. *Chin. Phys. B* **2022**, *31*, 060501. [CrossRef]
4. Jamil, A.A.; Tu, W.F.; Ali, S.W.; Terriche, Y.; Guerrero, J.M. Fractional-order PID controllers for temperature control: A review. *Energies* **2022**, *15*, 3800. [CrossRef]
5. Gómez-Echavarría, A.; Ugarte, J.P.; Tobón, C. The fractional Fourier transform as a biomedical signal and image processing tool: A review. *Biocybern. Biomed. Eng.* **2020**, *40*, 1081–1093. [CrossRef]
6. Prommee, P.; Pienpichayapong, P.; Manositthichai, N.; Wongprommoon, N. OTA-based tunable fractional-order devices for biomedical engineering. *AEU-Int. J. Electron. Commun.* **2021**, *128*, 153520. [CrossRef]
7. Arif, M.; Di Persio, L.; Kumam, P.; Watthayu, W.; Akgül, A. Heat transfer analysis of fractional model of couple stress Casson tri-hybrid nanofluid using dissimilar shape nanoparticles in blood with biomedical applications. *Sci. Rep.* **2023**, *13*, 4596.
8. Duran, S.; Durur, H.; Yavuz, M.; Yokus, A. Discussion of numerical and analytical techniques for the emerging fractional order murnaghan model in materials science. *Opt. Quantum Electron.* **2023**, *55*, 571. [CrossRef]
9. Müller, S.; Kästner, M.; Brummund, J.; Ulbricht, V. A nonlinear fractional viscoelastic material model for polymers. *Comput. Mater. Sci.* **2011**, *50*, 2938–2949. [CrossRef]
10. Tarasov, V.E. On history of mathematical economics: Application of fractional calculus. *Mathematics* **2019**, *7*, 509. [CrossRef]
11. Johansyah, M.D.; Supriatna, A.K.; Rusyaman, E.; Saputra, J. The Existence and Uniqueness of Riccati Fractional Differential Equation Solution and Its Approximation Applied to an Economic Growth Model. *Mathematics* **2022**, *10*, 3029. [CrossRef]
12. Johansyah, M.D.; Sambas, A.; Qureshi, S.; Zheng, S.; Abed-Elhameed, T.M.; Vaidyanathan, S.; Sulaiman, I.M. Investigation of the hyperchaos and control in the fractional order financial system with profit margin. *Partial Differ. Equ. Appl. Math.* **2024**, *9*, 100612. [CrossRef]
13. Johansyah, M.D.; Sambas, A.; Zheng, S.; Benkouider, K.; Vaidyanathan, S.; Mohamed, M.A.; Mamat, M. A novel financial system with one stable and two unstable equilibrium points: Dynamics, coexisting attractors, complexity analysis and synchronization using integral sliding mode control. *Chaos Solitons Fractals* **2023**, *177*, 114283. [CrossRef]
14. Dufera, T.T. Fractional Brownian motion in option pricing and dynamic delta hedging: Experimental simulations. *N. Am. J. Econ. Financ.* **2024**, *69*, 102017. [CrossRef]
15. Ma, P.; Najafi, A.; Gomez-Aguilar, J.F. Sub mixed fractional Brownian motion and its application to finance. *Chaos Solitons Fractals* **2024**, *184*, 114968. [CrossRef]
16. Guo, C.; Fang, S.; He, Y. Derivation and Application of Some Fractional Black–Scholes Equations Driven by Fractional G-Brownian Motion. *Comput. Econ.* **2023**, *61*, 1681–1705. [CrossRef]
17. Petcu, M.A.; Ionescu-Feleaga, L.; Ionescu, B.Ș.; Moise, D.F. A decade for the mathematics: Bibliometric analysis of mathematical modeling in economics, ecology, and environment. *Mathematics* **2023**, *11*, 365. [CrossRef]
18. Zhou, D.; Li, L.; Fakieh, B.; Ismail, R.I. User online consumption behaviour based on fractional differential equation. *Appl. Math. Nonlinear Sci.* **2022**, *7*, 415–424. [CrossRef]
19. Larni-Fooeik, A.; Sadjadi, S.J.; Mohammadi, E. Stochastic portfolio optimization: A regret-based approach on volatility risk measures: An empirical evidence from The New York stock market. *PLoS ONE* **2024**, *19*, e0299699. [CrossRef] [PubMed]
20. Inglada-Perez, L. A comprehensive framework for uncovering non-linearity and Chaos in financial markets: Empirical evidence for four major stock market indices. *Entropy* **2020**, *22*, 1435. [CrossRef] [PubMed]
21. Al Fahel, S.; Baleanu, D.; Al-Mdallal, Q.M.; Saad, K.M. Quadratic and cubic logistic models involving Caputo–Fabrizio operator. *Eur. Phys. J. Spec. Top.* **2023**, *232*, 2351–2355. [CrossRef]
22. Hegade, A.; Bhalekar, S. Stability analysis of Hilfer fractional-order differential equations. *Eur. Phys. J. Spec. Top.* **2023**, *232*, 2357–2365. [CrossRef]
23. Rahman, G.U.; Gómez-Aguilar, J.F.; Ahmad, D. Modeling and analysis of an implicit fractional order differential equation with multiple first-order fractional derivatives and non-local boundary conditions. *Eur. Phys. J. Spec. Top.* **2023**, *232*, 2367–2383. [CrossRef]
24. Zarraga, O.; Sarría, I.; García-Barruetabeña, J.; Cortés, F. An analysis of the dynamical behaviour of systems with fractional damping for mechanical engineering applications. *Symmetry* **2019**, *11*, 1499. [CrossRef]
25. Lozynskyy, A.; Chaban, A.; Perzyński, T.; Szafraniec, A.; Kasha, L. Application of fractional-order calculus to improve the mathematical model of a two-mass system with a long shaft. *Energies* **2021**, *14*, 1854. [CrossRef]
26. Zhang, X.; Boutat, D.; Liu, D. Applications of fractional operator in image processing and stability of control systems. *Fractal Fract.* **2023**, *7*, 359. [CrossRef]
27. Ma, Y.; Li, W. Application and research of fractional differential equations in dynamic analysis of supply chain financial chaotic system. *Chaos Solitons Fractals* **2020**, *130*, 109417. [CrossRef]
28. Stapleton, D.; Hanna, J.B.; Ross, J.R. Enhancing supply chain solutions with the application of chaos theory. *Supply Chain Manag. Int. J.* **2006**, *11*, 108–114. [CrossRef]
29. Ma, J.; Wang, H. Complexity analysis of dynamic noncooperative game models for closed-loop supply chain with product recovery. *Appl. Math. Model.* **2014**, *38*, 5562–5572. [CrossRef]
30. Xie, F.J.; Wen, L.Y.; Wang, S.Y.; Li, Y.F. Complex Characteristics and Control of Output Game in Cross-Border Supply Chains: A Perspective of Inter-Chain Competition. *Mathematics* **2024**, *12*, 313. [CrossRef]

31. Kocamaz, U.E.; Taşkın, H.; Uyaroğlu, Y.; Göksu, A. Control and synchronization of chaotic supply chains using intelligent approaches. *Comput. Ind. Eng.* **2016**, *102*, 476–487. [CrossRef]
32. Norouzi Nav, H.; Jahed Motlagh, M.R.; Makui, A. Robust controlling of chaotic behavior in supply chain networks. *J. Oper. Res. Soc.* **2017**, *68*, 711–724. [CrossRef]
33. He, Y.; Zheng, S.; Yuan, L. Dynamics of fractional-order digital manufacturing supply chain system and its control and synchronization. *Fractal Fract.* **2021**, *5*, 128. [CrossRef]
34. Yan, L.; Liu, J.; Xu, F.; Teo, K.L.; Lai, M. Control and synchronization of hyperchaos in digital manufacturing supply chain. *Appl. Math. Comput.* **2021**, *391*, 125646. [CrossRef]
35. Xu, X.; Kim, H.S.; You, S.S.; Lee, S.D. Active management strategy for supply chain system using nonlinear control synthesis. *Int. J. Dyn. Control* **2022**, *10*, 1981–1995. [CrossRef] [PubMed]
36. Cuong, T.N.; Kim, H.S.; You, S.S. Decision support system for managing multi-echelon supply chain networks against disruptions using adaptive fractional order control algorithm. *RAIRO-Oper. Res.* **2023**, *57*, 787–815. [CrossRef]
37. Hasan, A.; Akgül, A.; Farman, M.; Chaudhry, F.; Sultan, M.; De la Sen, M. Epidemiological analysis of symmetry in transmission of the Ebola virus with power law kernel. *Symmetry* **2023**, *15*, 665. [CrossRef]
38. Peng, Q.; Jian, J. Estimating the ultimate bounds and synchronization of fractionalorder plasma chaotic systems. *Chaos Solitons Fractals* **2021**, *150*, 111072. [CrossRef]
39. Podlubny, I. *Fractional Differential Equations, Mathematics in Science and Engineering*; Academic Press: New York, NY, USA, 1999.
40. Li, Y.; Chen, Y.Q.; Podlubny, I. Stability of fractional-order nonlinear dynamic systems: Lyapunov direct method and generalized Mittag-Lefflfler stability. *Comput. Math. Appl.* **2009**, *59*, 1810–1821. [CrossRef]
41. Kanwal, T.; Hussain, A.; Avci, I.; Etemad, S.; Rezapour, S.; Torres, D.F. Dynamics of a model of polluted lakes via fractalfractional operators with two different numerical algorithms. *Chaos Solitons Fractals* **2024**, *181*, 114653. [CrossRef]
42. Wang, D.Z.; Sun, L.S.; Sun, G.F. Fixed-time disturbance observer-based control for uncertainty systems applied to permanent-magnet speed control. *J. Electr. Eng. Technol.* **2024**, 1–14. [CrossRef]
43. Pan, W.; Li, T.; Sajid, M.; Ali, S.; Pu, L. Parameter identifification and the finite-time combination-combination synchronization of fractional-order chaotic systems with different structures under multiple stochastic disturbances. *Mathematics* **2022**, *10*, 712. [CrossRef]